WWW.IJRPR.COM

International Journal of Research Publication and Reviews

Journal homepage: www.ijrpr.com ISSN 2582-7421

DC Electrical Studies of $Ni_{0.65}Zn_{0.35}Fe_{2-x}In_xO_4$ ($0 \leq x \leq 0.24$) Prepared via Nitrate-Citrate Route

Ashok V. Humbe[1,2], B. N. Dole[1]

[1]Department of Physics, Dr. Babasaheb Ambedkar Marathwada University, Sub-campus, Dharashiv, Maharashtra - 413582
[2]Department of Physics, Dr. Babasaheb Ambedkar Marathwada University, Chhatrapati Sambhajinagar, Maharashtra – 431004

DOI : https://doi.org/10.5281/zenodo.15166499

ABSTRACT:

Nanosized $Ni_{0.65}Zn_{0.35}Fe_{2-x}In_xO_4$ with x = 0.0, 0.08, 0.16, and 0.24 spinel ferrites were prepared by using sol-gel auto combustion method. The DC resistivity studies of all the samples were carried out by two-probe technique as a function of temperature and the results revealed the semiconducting behavior. Moreover, Arrhenius plots indicate that as a function of In^{3+} doping the resistivity was found to increase. The activation energy determined using standard formula indicates increment with In^{3+}. Additionally, drift mobility and diffusion coefficient were computed using DC resistivity data. Both drift mobility and diffusion coefficient were found to decrease with In^{3+}, related to enhanced charge carrier concentration and production of cation vacancies respectively.

Keywords: Semiconducting nature, activation energy, charge carrier concentration, diffusion coefficient

Introduction:

Nanocrystalline spinel ferrites are crucial category of magnetic insulators in technology due to their magnetic characteristics, high electrical resistivity, and low eddy current and dielectric losses. These materials have extensive applications in microwave devices, high-density data storage devices, magnetic fluids, photocatalysts, gas sensors, targeted drug delivery systems, and more [1-5]. Several variables, such as the chemical composition, dopant, manufacturing procedure, cation dispersion, and other aspects, greatly influence all of these qualities. The properties and performance of nanocrystalline spinel ferrites are intricately linked to their chemical composition, dopants, synthesis methods, cation distribution, and other factors.

Nickel-zinc (Ni-Zn) spinel ferrites [6-8] and its replacement forms are very versatile and technologically important soft ferrite materials that have been extensively researched. They have a low conductivity, resulting in reduced eddy current losses. They also exhibit high electrochemical stability, catalytic activity, and other desirable characteristics. Furthermore, it exhibits a tunable electrical conductivity and an inverse spinel structure. Within the inverse spinel structure, the tetrahedral (A) sites are occupied by Fe^{3+} ions, while the octahedral [B] sites are equally occupied by divalent metal ions (Ni^{2+}) and Fe^{3+} ions. The angle A-O-B is closer to 180° compared to the angles B-O-B and A-O-A, resulting in a notable superexchange (anti-ferromagnetic) interaction between the A-B pair (Fe-Fe). Evidence indicates that the replacement of magnetic and nonmagnetic ions in the spinel structure leads to structural deformation and alters the Curie temperature.

Replacing Fe^{3+} ions with trivalent cations has been demonstrated to enhance the effectiveness of magnetic recording medium, computer memory storage, ferrofluids, catalytic activities, water treatment, hyperthermia, and other applications [9-11]. Trivalent indium (In^{3+}) is particularly noteworthy due to its dynamic electronic structure. The addition of In^{3+} ions into a Ni-Zn matrix can lead to the development of intriguing structural, electrical, and magnetic characteristics. In addition, the incorporation of In^{3+} ions can enhance electrical resistivity, leading to decreased dielectric and eddy current losses. This enables Ni-Zn spinel ferrites to be utilized across a broader range of frequencies. Inhibiting the grain formation, the mechanical strength can be enhanced and the coercivity can be reduced, resulting in a softer magnetic material that is more suitable for high frequency applications. Considering all the information provided, our current objective was to examine the impact of In^{3+} substitution in Ni-Zn spinel ferrite on its DC electrical properties.

Results and discussion

DC electrical resistivity:

Using a two-probe approach, the DC electrical resistivity was determined as a function of temperature in the range from ambient temperature to 850 K. A crucial characteristic of ferrites, especially for high-frequency applications, is its DC electrical resistivity. High resistivity is a need for high-frequency applications in order to compensate eddy current losses. Resistivity of spinel ferrites is influenced by porosity, particle size, density, and sintering temperature. Upon doping of In^{3+} ions, the observed values of DC resistivity of the original sample (Ni-Zn ferrite) had significantly enhanced.

It means that nano ferrites with such high resistivity has low eddy current losses, which is beneficial for their use in transformers, electromagnets, inductors, and other electronic components. On the basis of Verwey's hopping process, the observed behaviour of resistivity with In^{3+} can be explained. Verwey asserts that the conduction in ferrites originates from the hopping of electrons between the ions of the same element with different valence states (Fe^{3+} and Fe^{2+}) scattered over crystallographically equivalent sub-lattices, which causes polarization of the space charge. The concentration of Fe^{3+}/Fe^{2+} ion pairs at [B] sites and activation energy have a significant impact on the hopping probability. The concentration of Fe^{3+}/Fe^{2+} at the [B] site in parent sample $Ni_{0.65}Zn_{0.35}Fe_2O_4$ is regarded as being at its maximum. Due to preference of In^{3+} ions for occupying the [B] site, Fe^{3+} ions will temporarily migrate from this site. As a result, the ratio of Fe^{3+}/Fe^{2+} ions will decrease, which will diminish electron hopping and increase resistivity. Literature shows a similar response for doped spinel ferrites [12, 13]. Increased activation energy is another factor that can contribute to resistivity improvement.

Fig. 1 displays the Arrhenius plots of the log of resistivity (Ω-cm) versus 1000/T (k^{-1}), for all samples. The linear relation of DC resistivity contains two separate areas, as seen from Arrhenius plots. The conduction mechanisms and activation energies differ for each of these regions. The first is known as the ordered region and is a ferrimagnetic phase that typically obeys the hopping mechanism. The disordered region, the second region, is a part of the paramagnetic phase. Numerous researchers have observed that the change in slope, or Curie point in the Arrhenius plot, is connected with the magnetic order change from the ferrimagnetic phase to the paramagnetic phase. Here, the In^{3+} doping and its increase caused the Curie point to shift to lower temperature. Trivalent metal ions replaced spinel ferrites showed similar Curie point behaviour [14-16]. Due to the distribution of Fe^{3+} ions among the accessible (A) and [B] sites, the decreasing behaviour of the Curie temperature can be described in terms of the (A)-[B] exchange interaction. According to site occupancy, when the In^{3+} doped, In^{3+} entered to the (A) site pushing the Fe^{3+} ions out of the (A) site to the [B] site. Thus, the (A)-[B] exchange interaction become weaker, resulting in an increase in the moment distance between the (A) and [B] sites. The increase in lattice parameter with In^{3+} doping provides strong support for this. As a result, the Curie temperature of prepared nanocrystalline spinel ferrites has lowered due to In^{3+} doping. Moreover, Fig. 1 clearly shows that as temperature increases, the DC electrical resistivity falls, indicating semiconductor behaviour. Similar temperature-dependent DC electrical resistivity behaviour for nanocrystalline spinel ferrites has been documented [17-19]. Due to increase in thermal mobility of charge carriers as temperature rises, the DC electrical resistivity decreases as a function of temperature. As a result, DC electrical resistivity reduces as temperature rises.

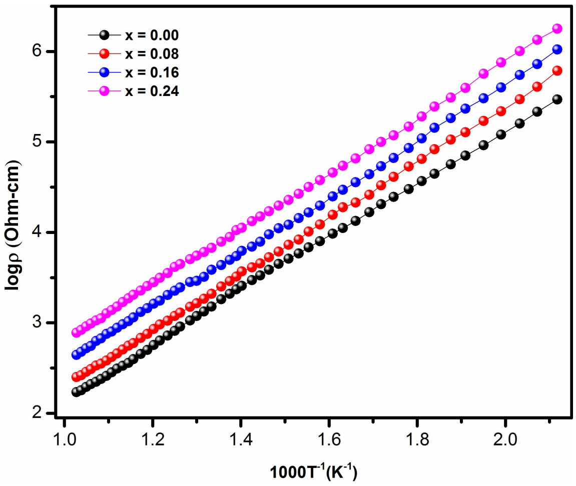

Fig. 1: DC resistivity plots of $Ni_{0.65}Zn_{0.35}Fe_{2-x}In_xO_4$ (x = 0.00, 0.08, 0.16 and 0.24)

Table 1 list the activation energy estimated using the following relation, which ranges from 0.4498 to 0.6361 eV. Activation energy is the energy required to free an electron from one ion, enabling it to jump to a neighboring ion, thereby contributing to electrical conductivity.

$$\rho = \rho_0 \, e^{\frac{\Delta E}{KT}} \qquad \ldots 1$$

In the studied temperature range, activation energies were determined for both regions: the ferrimagnetic region which is a low-temperature region and the high-temperature region is known as paramagnetic region. These values were calculated from the slope of the plots of DC electrical resistivity. With In^{3+} ions, the activation energy rises in both paramagnetic and ferrimagnetic regions. When comparing the two activation energies, it is clear that the activation energy of ferrimagnetic region is lower than that of the paramagnetic region. The lower activation energy in the ferrimagnetic region indicates magnetic disordering due to a decrease in the charge carriers concentration. This demonstrates how the magnetic phase variation affects the conduction.

Drift mobility (μ_d): The following relation was used to compute the drift mobility.

$$\mu_d = \frac{1}{ne\rho} \qquad \ldots 2$$

where e is the charge on the electron, n is the charge carrier concentration, d is the drift mobility, and ρ is the resistivity. A standard relation [16] was used to calculate the charge carrier concentration for each sample, and the results are shown in Table 1. With In^{3+}, it was discovered that the concentration of charge carriers vary from 7.41×10^{22} to 6.56×10^{22} atoms /cm^3. The observed values of drift mobility range from 3.77×10^{-5} to 1.52×10^{-6} which are very small. Other researchers have previously observed such low values of drift mobility for nanocrystalline spinel ferrites [20]. Fig. 2 displays the graph of drift mobility (cm^2/Vs) with temperature (K). Fig. 2 shows that when temperature rises, the mobility of the charge carriers increases. As In^{3+} concentration increases, it is observed that the drift mobility reduces, which can be explained by an increase in charge carrier concentration.

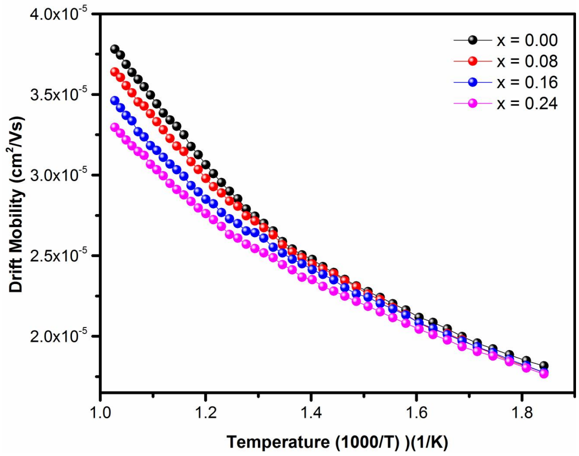

Fig. 2: Drift mobility plots of $Ni_{0.65}Zn_{0.35}Fe_{2-x}In_xO_4$ (x = 0.00, 0.08, 0.16 and 0.24)

Sample	**Activation Energies**			**n×10^{22} (atoms/cm^3)**	**D (cm^2/s)**		
	E_p (eV)	**E_f (eV)**	**ΔE (eV)**		**At 473k**	**At 723k**	**At 973k**
0.00	0.5077	0.0579	0.4498	7.41	1.23×10^{-7}	3.07×10^{-7}	6.23×10^{-7}
0.08	0.5534	0.0827	0.4707	7.15	1.17×10^{-7}	2.95×10^{-7}	5.80×10^{-7}
0.16	0.6757	0.1327	0.5430	6.83	1.12×10^{-7}	2.77×10^{-7}	5.26×10^{-7}
0.24	0.8509	0.2148	0.6361	6.56	1.08×10^{-7}	2.57×10^{-7}	4.81×10^{-7}

Diffusion coefficient (D): The diffusion coefficient for each sample was calculated using the relation given below as a function of temperature.

$$D = \frac{\sigma k_B T}{Ne^2} \quad \ldots 10$$

Where conductivity (σ), Boltzmann constant (k_B), temperature (T), number of atoms per cubic centimeter (N), and charge (e) are the variables. Table 1 lists the computed diffusion coefficient values for each sample at three distinct temperatures. The diffusion coefficient rises as temperature rises because conductivity increases. On the other hand, for three different temperatures, the diffusion coefficient decreases with In^{3+}. This is explained by the substitution of In^{3+} in the sublattice, which results in the production of cation vacancies and a decrease in oxygen vacancies.

Conclusion

The DC electrical resistivity with temperature and In^{3+} doping concentration was found to increase, which exhibits semiconducting nature. The activation energy enhanced with In^{3+} doping. Moreover, In^{3+} doping enhanced charge carrier concentration, reducing drift mobility. Additionally, diffusion coefficient decreased with In^{3+} doping.

References

[1] A.V. Humbe, J.S. Kounsalye, S.B. Somvanshi, A. Kumar, K. Jadhav, Materials Advances, 1 (2020) 880-890.

[2] H. Qin, Y. He, P. Xu, D. Huang, Z. Wang, H. Wang, Z. Wang, Y. Zhao, Q. Tian, C. Wang, Advances in Colloid and Interface Science, 294 (2021) 102486.

[3] A. Sagar, S. Bhardwaj, A. Gupta, H. Tripathi, R. Shukla, Interactions, 245 (2024) 86.

[4] S.J. Salih, W.M. Mahmood, Heliyon, 9 (2023).

[5] P. Thakur, S. Taneja, D. Chahar, B. Ravelo, A. Thakur, Journal of Magnetism and Magnetic Materials, 530 (2021) 167925.

[6] M.A. Siddiqui, M. Khalid, M. Younas, J.K. Khan, A. Ahmed, M. Ashiq, M. mana Al-Anazy, I. Boukhris, S. Ismail, K. Naz, Ceramics International, 50 (2024) 43947-43960.

[7] D. Fei, Y. Guo, J. Zhou, J. Tao, N. Chen, Z. Yao, X. Tao, L. Duan, J. Liu, B. Ouyang, Materials Research Bulletin, 173 (2024) 112662.

[8] W. Li, B. Dai, Z. Li, H. Yang, G. Liu, F. Xu, Journal of Materials Science: Materials in Electronics, 35 (2024) 541.

[9] G. Nandhini, M. Shobana, Materials Today Communications, 39 (2024) 109046.

[10] B. Sahu, K. Ramesh, D. Venkatesh, S.L. Pandrangi, P. Chittineedi, B.P. Singh, Materials Chemistry and Physics, (2025) 130749.

[11] W. Al-Ghamdi, H. Almaghamsi, N. Basfer, Ceramics International, 50 (2024) 6725-6734.

[12] K. Farooq, M. Irfan, M.N. Akhtar, R.T. Rasool, M. Mahmoud, A. Almohammedi, G.A. Ashraf, M.A. Khan, Ceramics International, 50 (2024) 33050-33064.

[13] A. Hakeem, T. Alshahrani, G. Muhammad, M. Alhossainy, A. Laref, A.R. Khan, I. Ali, H.M.T. Farid, T. Ghrib, S.R. Ejaz, Journal of Materials Research and Technology, 11 (2021) 158-169.

[14] B. Kar, P. Kumar, S. Panigrahi, D.P. Sahu, S. Mishra, Ceramics International, 50 (2024) 49587-49599.

[15] P.G. Undre, A.V. Humbe, J.S. Kounsalye, A. Kumar, R.V. Kathare, K.M. Jadhav, Journal of Inorganic and Organometallic Polymers and Materials, 33 (2023) 3372-3388.

[16] A.V. Humbe, P.B. Kharat, A.C. Nawle, K.M. Jadhav, Journal of Materials Science: Materials in Electronics, 29 (2018) 3467-3481.

[17] T. Reddy, S.R. Akepati, V. Nagalakshmi, D.J. Rao, R. Madaka, Inorganic Chemistry Communications, 165 (2024) 112480.

[18] M. Raju, P. Shanmukhi, G.U. Reddy, N. Murali, T.W. Mammo, M. Kahsay, G. Hagos, T. Aregai, B. Swarnalatha, D. Parajuli, Inorganic Chemistry Communications, 163 (2024) 112274.

[19] R.B. Sathe, C.U. Narayankar, N. Abderrahim, P. Kumar, J.S. Ghodake, R.H. Patil, S.H. Khoreem, A. Dinesh, M. Ayyar, H. Elhouichet, Inorganic Chemistry Communications, 170 (2024) 113408.

[20] N. Abu-Elsaad, S. Mazen, A. Nawara, Journal of Alloys and Compounds, 856 (2021) 157794.